Precise intensity correlation measurement for atomic resonance fluorescence from optical molasses

Kazuyuki Nakayama[1], Yutaka Yoshikawa[1,2], Hisatoshi Matsumoto[1,2], Yoshio Torii[1,2], and Takahiro Kuga[1,2]

[1]*PRESTO, CREST, Japan Science and Technology Agency, 4-1-8 Honcho, Kawaguchi, Saitama, Japan.*

[2]*Institute of Physics, University of Tokyo, 3-8-1, Meguro-ku, Komaba, Tokyo 153-8902, Japan.*

nakayama@photon.c.u-tokyo.ac.jp

Abstract: We measured the intensity correlation of true thermal light scattered from cold atoms in an optical molasses. Using a single-mode fiber as a transverse mode filter, measurement with maximally high spatial coherence was realized, allowing us to observe ideal photon bunching with unprecedented precision. The measured intensity correlation functions showed a definite bimodal structure with fast damped oscillation from the maximum value of $2.02(3)$ and slow monotonic decay toward unity. The oscillation can be understood as an interference between elastic and inelastic scattering fields in resonance fluorescence.

OCIS codes: (020.3320) Laser cooling; (030.5260) Photon counting; (270.5290) Photon statistics

References and links

1. R. Hanbury Brown and R. Q. Twiss, "Correlation between photons in two coherent beams of light," Nature (London) **177,** 27–29 (1956).
2. D. Kleppner, "Hanbury Brown's steamroller," Phys. Today **61,** 8–9 (2008).
3. R. Loudon, *The Quantum Theory of Light* (Oxford Univ. Press, London, 1983).
4. F. T. Arecchi, E. Gatti, and A. Sona "Time distribution of photons from coherent and Gaussian sources," Phys. Lett. **20,** 27–29 (1966).
5. B. L. Morgan, and L. Mandel, "Measurement of Photon Bunching in a Thermal Light Beam," Phys. Rev. Lett. **16,** 1012–1015 (1966).
6. D. Zhang, Y. H. Zhai, L. A. Wu, and X. H. Chen, " Correlated two-photon imaging with true thermal light," Opt. Lett. **30,** 2354–2356 (2005).
7. C. Jurczak, K. Sengstock,amazon R. Kaiser, N. Vansteenkiste, C. I. Westbrook, and A. Aspect, "Observation of intensity correlations in the fluorescence from laser cooled atoms," Opt. Commun. **115,** 480–484 (1995).
8. C. Jurczak, B. Desruelle, K. Sengstock, J.-Y. Courtois, C. I. Westbrook, and A. Aspect, "Atomic Transport in an Optical Lattice: An Investigation through Polarization-Selective Intensity Correlations," Phys. Rev. A **77,** 1727–1730 (1996).
9. S. Bali, D. Hoffmann, J. Simán, and T. Walker, "Measurements of intensity correlations of scattered light from laser-cooled atoms," Phys. Rev. A **53,** 3469–3472 (1996).
10. R. Stites, M. Beeler, L. Feeney, S. Kim, and S. Bali, "Sensitive measurement of radiation trapping in cold-atom clouds by intensity correlation detection," Opt. Lett. **29,** 2713–2715 (2004).
11. H. J. Kimble, and L. Mandel, "Theory of resonance fluorescence," Phys. Rev. A **13,** 2123–2144 (1976).
12. M. O. Scully, and M. S. Zubairy, *Quantum Optics* (Cambridge Univ. Press, Cambridge, 1997).
13. B. Chu, *Laser Light Scattering* (Academic Press, San Diego, CA, 1991).
14. C. I. Westbrook, R. N. Watts, C. E. Tanner, S. L. Rolston, W. D. Phillips, P. D. Lett, and P. L. Gould, "Localization of atoms in a three-dimensional standing wave," Phys. Rev. Lett. **65,** 33–36 (1990).

#123497 - $15.00 USD Received 29 Jan 2010; revised 9 Feb 2010; accepted 9 Feb 2010; published 15 Mar 2010

15. B. R. Mollow, "Power Spectrum of Light Scattered by Two-Level Systems," Phys. Rev. **188,** 1969–1975 (1969).
16. B. Gao, "Effects of Zeeman degeneracy on the steady-state properties of an atom interacting with a near-resonant laser field: Resonance flourescence," Phys. Rev. A **50,** 4139–4156 (1994).
17. M. Beeler, R. Stites, S. Kim, L. Feeney, and S. Bali, "Sensitive detection of radiation trapping in cold-atom clouds," Phys. Rev. A **68,** 013411 (2003).
18. I. R. Senitzky, "Quantum-Mechanical Saturation in Resonance Fluorescence," Phys. Rev. A **6,** 1171–1174 (1972).
19. G. S. Agarwal, A. C. Brown, L. M. Narducci, and G. Vetri, "Collective atomic effects in resonance fluorescence," Phys. Rev. A **15,** 1613–1624 (1977).
20. S. V. Lawande, R. R. Puri, and S. S. Hassan, "Non-resonant effects in the fluorescent Dicke model I. Exact steady state analysis," J. Phys. B: At. Mol. Phys. **14,** 4171–4189 (1981).
21. S. S. Hassan, G. P. Hildred, R. R. Puri, and S. V. Lawande, "Non-resonant effects in the fluorescent Dicke model II. Semiclassical and quantal results," J. Phys. B: At. Mol. Phys. **15,** 1029–1049 (1982).
22. O. Assaf and E. Akkermans, "Intensity Correlations and Mesoscopic Fluctuations of Diffusing Photons in Cold Atoms," Phys. Rev. Lett. **98,** 083601 (2007).

1. Introduction

Intensity correlation measurement (ICM) of light was first demonstrated by Hanbury Brown and Twiss in 1956 [1] to measure the angular diameter or apparent size of radio stars, which nowadays finds numerous applications in the fields of quantum optics, nuclear physics, and cold atoms [2]. Generally, ICM is accomplished by monitoring temporal fluctuations of light intensity $I(t)$ and deriving the second-order correlation function by [3]

$$g^{(2)}(\tau) = \frac{\langle I(t)I(t+\tau)\rangle}{\langle I(t)\rangle^2}. \tag{1}$$

For coherent light, $g^{(2)}(\tau)$ is expected to be unity for any τ, implying no correlation between successive incoming photons. In contrast, for thermal (chaotic) light emitted from a number of independent radiators, $g^{(2)}(0)$ is predicted to be 2, which represents strong bunching of photons. Arecchi *et al*. [4] confirmed this prediction experimentally with quasi-thermal light prepared by passing a He-Ne laser through a rotating ground-glass disc. Also, in previous experiments, intensity correlation of true thermal light, such as fluorescence from atomic beams [5] and light from a discharge lamp [6], has been measured, and photon bunching at $\tau \sim 0$ was definitely observed. However, to the best of our knowledge, no experiments have demonstrated ideal photon bunching [$g^{(2)}(0) = 2$], probably due to the lack of time resolution and imperfect spatial coherence in the measurements.

In the 1980s, techniques for laser cooling and trapping developed rapidly and allowed the use of atomic fluorescence as a probe of the dynamic and optical properties of atoms in laser fields [7–10]. In these works, however, measured $g^{(2)}(0)$ values were still as low as $1.1-1.3$; nevertheless, the time resolution requirement was greatly relaxed because of slow atomic motion. Stites *et al*. [10] attributed this degradation to radiation trapping in an atomic cloud and successfully reproduced the decrease in $g^{(2)}(0)$ in numerical calculations. However, the calculated correlation time did not agree with the experimental results, and, to our knowledge, no reasonable explanation has been given so far. Thus, measuring $g^{(2)}(\tau)$ for fluorescence from cold atoms and establishing a proper theoretical model are still important subjects in atomic physics and quantum optics.

In this paper, we report on the measurement of $g^{(2)}(\tau)$ for fluorescence from laser-cooled atoms with unprecedented high precision. In contrast to previous works [7–10], we adopted continuously loaded atoms in an optical molasses as a light source and developed a novel ICM scheme with a single-mode fiber. The measured $g^{(2)}(\tau)$ showed not only ideal photon bunching [$g^{(2)}(0) = 2$], but also a characteristic bimodal structure originating from inelastic light scattering of atoms. These results were in excellent agreement with calculations based on the basic theory of atomic resonance fluorescence [11, 12].

#123497 - $15.00 USD Received 29 Jan 2010; revised 9 Feb 2010; accepted 9 Feb 2010; published 15 Mar 2010

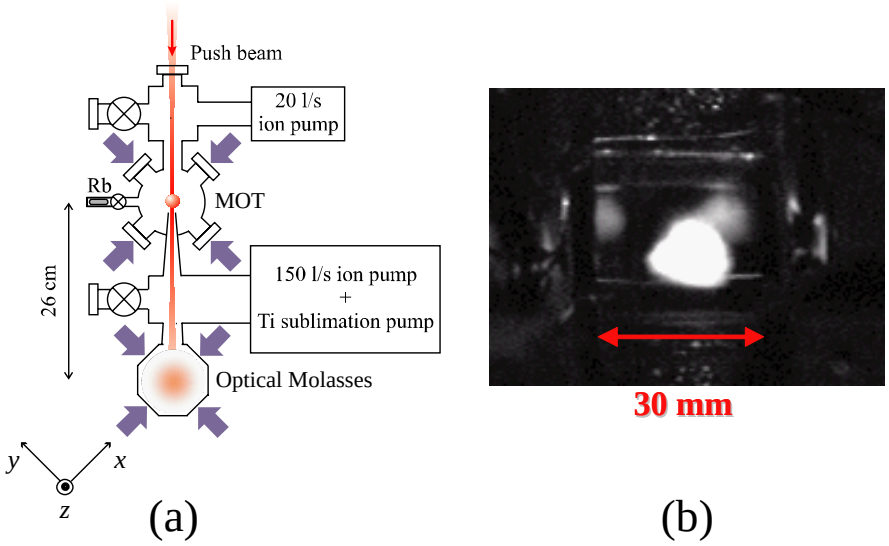

Fig. 1. Schematic diagram of the setup for optical molasses. (a) Atoms captured in the MOT were pushed out by a weak laser beam and continuously transferred to the optical molasses through a differential pumping tube 5 mm in diameter. (b) Fluorescence image of the optical molasses. The steady state number of atoms contained in the optical molasses was 3×10^9. Movie of the optical molasses loading (Media 1).

This paper is organized as follows. In section 2, we present the experimental setup for producing an optical molasses, with which high-intensity true thermal light can be obtained continuously. We also describe the detection scheme with a single-mode fiber, focusing particularly on achievable spatial coherence in ICM. Section 3 presents the results and discussion. We analyze and interpret the measured $g^{(2)}(\tau)$ in terms of atomic resonance fluorescence and its spectral density distribution. Finally, a summary is given in section 4.

2. Experiment

2.1. Continuously Loaded Optical Molasses

A large number of cold atoms are necessary to perform high-precision ICM of light scattered from cold atoms. Sources of cold atoms used in previous experiments were based on a vapor-cell magneto-optical trap (MOT) [7, 9, 10]: a transient optical molasses was created by switching off the magnetic field of the MOT periodically. The figure of merit of the experiment is the time-averaged atom number, given by $N\eta$, where N and η are the typical atom number and duty cycle, respectively. The typical parameters for previous experiments were $N \sim 10^7$ and $\eta \sim 0.01$. Therefore, $N\eta$ was $\sim 10^5$; the total count rate was not sufficient for precise ICM.

To solve this problem, we have adopted a continuously loaded optical molasses. Figure 1(a) shows the experimental setup for the optical molasses. The vacuum chamber consisted of two regions vertically separated by 26 cm. The upper trap was a standard MOT, which worked as a source of cold atoms. The background pressure of Rb was kept as high as $\sim 10^{-7}$ Pa so that the atoms accumulated efficiently in the MOT. The lower molasses region was located inside an octagonal glass cell evacuated by a 150-l/s ion pump and a titanium sublimation pump to keep an ultrahigh-vacuum (UHV) of $\sim 10^{-9}$ Pa. This UHV condition is critical to suppress background-gas collisions and increase the number of atoms in the molasses. To stabilize an

#123497 - $15.00 USD Received 29 Jan 2010; revised 9 Feb 2010; accepted 9 Feb 2010; published 15 Mar 2010

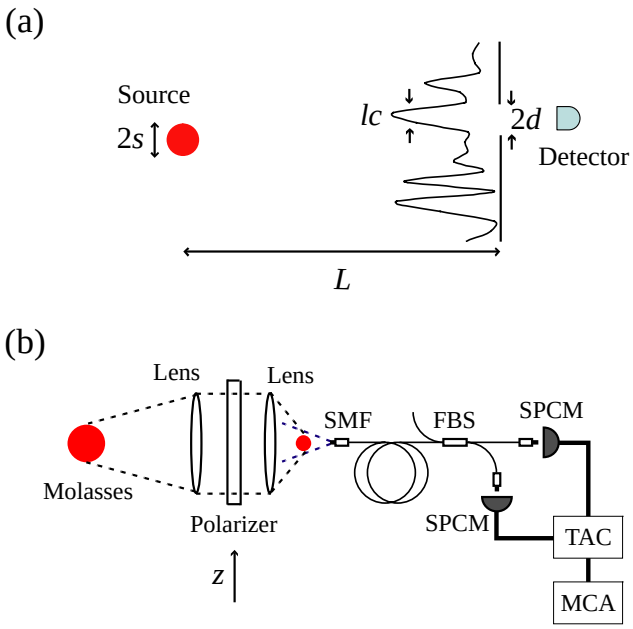

Fig. 2. Optical molasses detection setup. (a) Relationships between the optical setup and correlation length. (b) Schematic diagram of measurement setup for the second-order intensity correlation function. A facet of a single-mode fiber was directed to the reduced image of the molasses and the mode-filtered light was led to a photon correlator. SMF: single-mode fiber, FBS: fiber beam splitter, SPCM: single photon counting module, TAC: time-to-amplitude converter, and MCA: multi-channel analyzer.

optical molasses, three pairs of square coils were wrapped around the glass cell and reduced the residual magnetic field to less than 10 mG over the molasses volume. To load the atoms into the lower molasses region, an 11-μW push beam was continuously applied from the upper side of the MOT, with the beam focus adjusted onto the trap center. The atoms in the MOT were then pushed out by radiation pressure and sent to the lower UHV region through a differential pumping tube 5 mm in diameter. The flux and longitudinal velocity of the resulting atomic beam were measured to be $\sim 2\times 10^9$ s^{-1} and 14 m/s, respectively. The slow atomic beams were decelerated and recaptured by circularly polarized cooling beams in a six-beam configuration. The counter-propagating (x, y, z)-axis beams were (25, 25, 20) mm in diameter with (10, 10, 3.4) mW in power (the coordinate axes were defined along the cooling beams). The laser frequency detuning δ was changed in the experiment from -20 MHz to -5 MHz for the cooling transition $|5S_{1/2}; F=2\rangle \rightarrow |5P_{3/2}; F=3\rangle$ of ^{87}Rb. A 5-mW repump laser was mixed with one of the z-axis beams. Figure 1(b) shows a movie of the optical molasses loaded in the glass cell. The number of atoms in the optical molasses saturates at 3×10^9 after 10 s of loading. For our experiment, η was almost 1; therefore, $N\eta$ was $\sim 10^9$, which was 10^4 times larger than that in previous works [7–10].

#123497 - $15.00 USD Received 29 Jan 2010; revised 9 Feb 2010; accepted 9 Feb 2010; published 15 Mar 2010

2.2. *Intensity Correlation Measurement with a Single-mode Fiber*

The light field scattered from cold atoms is well modeled as a thermal light source. In this case, $g^{(2)}(\tau)$ can be expressed as

$$g^{(2)}(\tau) = 1 + \beta\,|g^{(1)}(\tau)|^2, \tag{2}$$

where $g^{(1)}(\tau)$ is the first-order intensity correlation function. The factor β is the spatial coherence factor, which is related to the correlation length $l_c = \lambda L/(\pi s)$ at the position of the detector. Here λ, s, and L are the wavelength of the scattered light, radius of the light source, and distance between light source and detector, respectively. Physically l_c corresponds to the length scale of the speckle pattern [Fig. 2(a)]. If the radius of the detector d is smaller than l_c, β is 1; there are no degradation of the intensity correlation between successive incoming photons [13]. In contrast, if $d \gg l_c$, β is limited to $(l_c/d)^2$. This suggests that to measure ideal photon bunching of the scattered light, one must decrease the size of either the source or detector.

In the present experiment, we adopted a detection scheme with a single-mode fiber [see Fig. 2(b)]. The facet of the single-mode fiber was directed to the light source with no coupling lens. The numerical aperture (NA) of the single-mode fiber is given as $\theta_{\mathrm{NA}} = 2\lambda/(\pi d_{\mathrm{MF}})$, where d_{MF} is the mode-field diameter corresponding to the detector diameter $2d$. When the source area πs^2 is smaller than the field of view of the fiber mode $\pi(L\theta_{\mathrm{NA}})^2$, photons coupled into the fiber can be treated as a pure single mode and automatically satisfies the maximal spatially coherent condition $\beta \approx 1$. We note that the multi-mode fibers with large active apertures ($50 \sim 100\ \mu$m) do not have this advantage. Figure 2(b) shows the measurement setup. In the experiment, a 2-cm molasses was imaged 2 cm away from the fiber facet ($d_{\mathrm{MF}} = 4.5\mu$m) with a pair of lenses (magnification factor of 1/7.5). A linear polarizer, oriented along the z direction, was inserted between the imaging lenses. The coupled light was split with a 50/50 inline fiber beam splitter, and $g^{(2)}(\tau)$ was measured with two single photon counting modules, a time-to-amplitude converter and multi-channel analyzer. The time window was 5 μs with 2.5-ns-wide time bins. The typical signal count rate was 2×10^4 s^{-1}, and the background count rate was 2×10^2 s^{-1}, owing to both dark counts and stray light. The signal count rate was low enough to eliminate double-counting errors. This was verified by measuring $g^{(2)}(\tau)$ with a weak laser that yielded the same count rate of 2×10^4 s^{-1}, giving $g^{(2)}(\tau) = 1$ within the statistical uncertainty. A single correlation measurement took about eight hours with a total of 10^7 counts, which was large enough to obtain a sufficiently low statistical uncertainty.

3. Results and discussion

Figures 3(a) and (b) show the measured $g^{(2)}(\tau)$ for various detunings. The average $g^{(2)}(0)$ was $2.02(3)$ that is the first observation of the ideal theoretical value for true thermal light, which is the most significant result in this paper. Remarkably, the measured $g^{(2)}(\tau)$ showed a definite bimodal structure with a slow monotonic decay [Fig. 3(a)] determined mainly by the temperature of the cold atoms and a fast damped oscillation [Fig. 3(b)] resulting from the interference between the coherent Rayleigh scattering component and the incoherent resonance fluorescence component.

The first-order correlation function for light scattered from atoms at temperature T excited by a near-resonant light field is given as

$$g^{(1)}(\tau) = g_{\mathrm{D}}^{(1)}(\tau)\cdot g_{\mathrm{H}}^{(1)}(\tau), \tag{3}$$

where $g_{\mathrm{D}}^{(1)}(\tau)$ and $g_{\mathrm{H}}^{(1)}(\tau)$ are referred to as the inhomogeneous and homogeneous component, respectively. This results from the assumption that the frequency spectrum of scattered light is

#123497 - $15.00 USD Received 29 Jan 2010; revised 9 Feb 2010; accepted 9 Feb 2010; published 15 Mar 2010

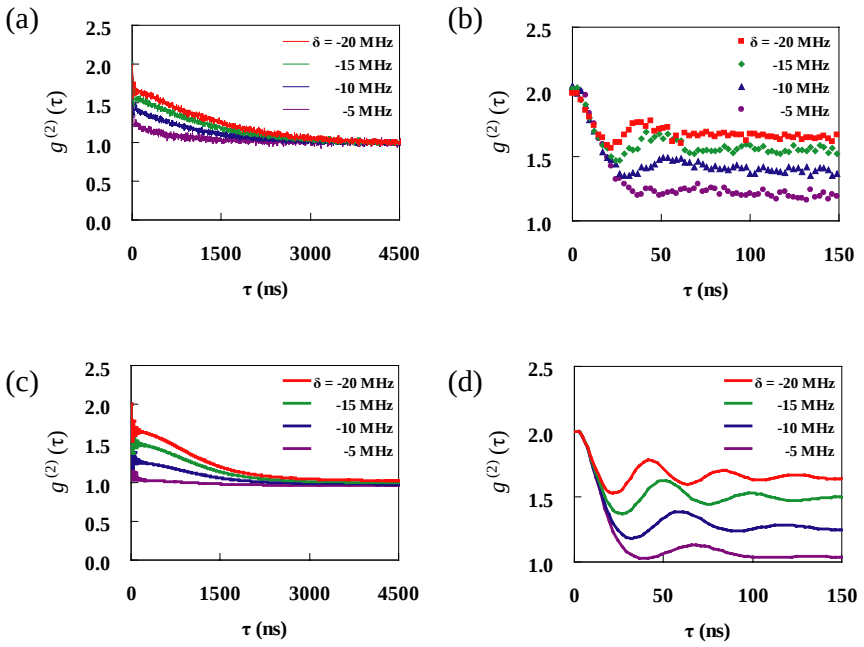

Fig. 3. Measurements of the second-order intensity correlation as a function of delay time for various detunings. (a) Long-time decay of the correlation function. The damping time was determined by the temperature of the cold atoms. (b) Short-time decay of the correlation function. A fast damped oscillation was observed with a short decay time determined by the lifetime of the excited state. (c), (d) Theoretical simulations based on Eqs. (2)−(5).

determined by the convolution of the Doppler profile and the frequency spectrum of atoms at rest [9]. The inhomogeneous component $g_{\rm D}^{(1)}(\tau)$ is the sum of the Doppler contribution from the six laser beams traveling in the x, y, and z directions [9, 14].

$$g_{\rm D}^{(1)}(\tau) = \sum_{i=1}^{6} a_i \exp\left(-\alpha_i \frac{\sigma^2\tau^2}{2}\right). \tag{4}$$

The parameter $\sigma = q(k_{\rm B}T/M)^{1/2}$ is the standard Doppler width, where q, $k_{\rm B}$, and M are the wave number of the laser light, the Boltzmann constant, and the mass of the atom, respectively. Here, $\alpha_j = 2(1-\cos\theta_j)$ gives the dependence of the Doppler shift on the angle θ_j between the observation direction and the propagation direction of the j-th laser beam. For our geometry, $\alpha_j = 2-2^{1/2}$ for the beams applied from the $+x$ and $+y$ directions, $2+2^{1/2}$ for the $-x$ and $-y$ directions, and 2 for the $\pm z$ directions. The normalized weighting coefficients a_j are determined by the intensity of each laser beam and are also proportional to the dipole radiation pattern. In our experiment, $a_j = 0.21$, 0.21, and 0.08 for the beams in the $\pm x$, $\pm y$, and $\pm z$ directions, respectively.

The homogeneous component $g_{\rm H}^{(1)}(\tau)$ [11] is

$$g_{\rm H}^{(1)}(\tau) = \frac{\delta^2+\gamma^2}{\delta^2+\gamma^2+\Omega^2/2} - \frac{\Omega^2}{2}\sum_{j\neq k\neq l}^{3} \frac{p_j+2\gamma}{p_j(p_j-p_k)(p_j-p_l)}\exp(p_j\tau), \tag{5}$$

#123497 - $15.00 USD Received 29 Jan 2010; revised 9 Feb 2010; accepted 9 Feb 2010; published 15 Mar 2010

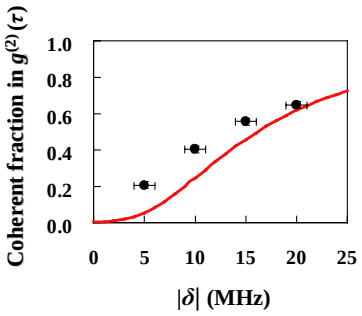

Fig. 4. Coherent fraction of the total scattered light in $g^{(2)}(\tau)$ for several detunings. Circles are experimental data, and red solid line is the theoretical curve $R(\delta)$, representing the ratio of the coherent Rayleigh scattered light to the total scattered light.

where Ω and γ are the Rabi frequency and the half natural linewidth of atoms, respectively. The complex eigenvalues p_1, p_2, and p_3 are roots of the cubic equation $p^3+4\gamma p^2+(5\gamma^2+\delta^2+\Omega^2)\,p+(2\gamma^2+2\delta^2+\Omega^2)\,\gamma=0$. The first term of Eq. (5) is the coherent Rayleigh scattering component. The second term consists of three incoherent components corresponding to the Mollow triplet in the frequency domain [15]. The real and imaginary parts of the complex eigenvalues correspond to the decay rate and oscillation frequency of the correlation function, respectively, which will be discussed later. For our experimental condition, we obtain one imaginary eigenvalue p_1 and one pair of complex conjugate eigenvalues p_2 and p_3. We also introduce the effective Rabi frequency $\Omega_{\rm eff}(\delta)$ as the real part of the complex eigenvalues, which will be used in the following analysis.

Figures 3(c) and (d) show numerical simulations of $g^{(2)}(\tau)$ based on Eqs. (2)$-$(5). The temperature used in the simulations was obtained by an independent standard time-of-flight technique [54(6) μK], measured with $\delta=-20$ MHz. Actually the temperature of cold atoms changes with δ, although we are not interested with the temperature in the present work. However the simulations reproduced the characteristic feature of the experiment well. The long-term correlation (the coherent contribution excluding the damped oscillation) in 3(b) decreased with small detunings. This can be understood by considering the ratio of the coherently scattered component to the total scattered light $R(\delta)$ written as

$$R(\delta)=\left(\frac{\delta^2+\gamma^2}{\delta^2+\gamma^2+\Omega^2/2}\right)^2. \tag{6}$$

Figure 4 shows the coherent fraction of the scattered light for several detunings. The circles are experimental data, and the red solid line is the theoretical curve $R(\delta)$. The discrepancy between the experimental results and the theoretical curve for small detunings is mainly due to the Raman contribution [16], which is not considered in the above analysis.

Figure 5(a) shows the dependence of the frequency of the fast damped oscillation on $|\delta|$. This dependence can be understood simply in terms of the spectral density obtained from the Fourier transform of $g^{(1)}(\tau)$. Figure 5(b) shows the theoretical curve of the spectral density of the fluorescence for several detunings; the horizontal axis is the relative frequency, defined as the difference frequency between the fluorescence and the resonant frequency of atoms. The spectral density is composed of a sharp spike, corresponding to the coherent Rayleigh scattering component, and the incoherent Mollow triplet symmetrically separated by $\Omega_{\rm eff}(\delta)$. The oscillation structure in $g^{(2)}(\tau)$ is explained as the interference between the central coherent

#123497 - $15.00 USD Received 29 Jan 2010; revised 9 Feb 2010; accepted 9 Feb 2010; published 15 Mar 2010

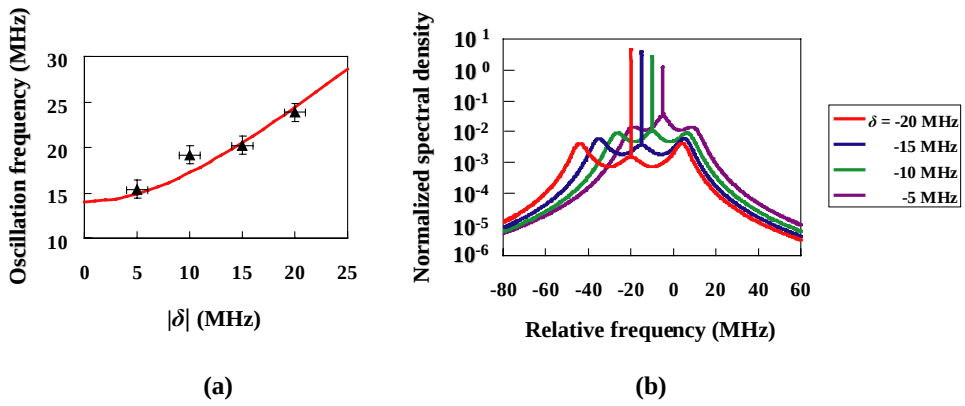

Fig. 5. (a) Oscillation frequency in $g^{(2)}(\tau)$. Triangles are experimental points, and red solid line is the effective Rabi frequency $\Omega_{\rm eff}(\delta)$. (b) Theoretical curve of the spectral density of the fluorescence for several detuning parameters versus the relative frequency.

component and the incoherent side component of the Mollow triplet. The triangles in Fig. 5(a) are experimental data, and the red solid line is $\Omega_{\rm eff}(\delta)$. The oscillation frequency was consistent with $\Omega_{\rm eff}(\delta)$ assuming the mean saturation intensity of 3.4 mW/cm^2, and a random distribution of Zeeman sublevels of atoms.

In this experiment, an optical density (OD) of the sample was on the order of unity, and $g^{(2)}(\tau)$ safely showed the ideal value of 2. However, this result is in clear contrast to the theoretical prediction proposed by Beeler *et al*. [17]; they considered multiple photon scattering in an optically dense sample and studied its influence on ICM, concluding that even an OD of 0.4 leads to drastic decrease of $g^{(2)}(0)$. Furthermore, the experimental result that seemed to support this prediction was also reported [10]. To identify this effect we also measured $g^{(2)}(\tau)$ with an optically thick MOT (OD of 3). Although the damping time was shorter, due to the inhomogeneous magnetic field and higher temperature of MOT, no substantial decrease of correlation depending on an OD, appeared in the experimental result. Thus, we conclude that the simple resonance fluorescence model, which does not include the multiple scattering effect, is sufficient to explain the intensity correlation of cold-atom fluorescence. One reason for the discrepancy to the previous report [10] may be due to the lack of time resolution in the previous measurement ($50-100$ ns), which smooths out the sharp structure of $g^{(2)}(\tau)$ in a short time range.

4. Conclusion

We have precisely measured the intensity correlation function $g^{(2)}(\tau)$ for true thermal light scattered from cold atoms in an optical molasses. We observed strong photon bunching [$g^{(2)}(0) = 2.02(3)$] and rapid damped oscillation due to the interference between the coherent Rayleigh scattering component and the incoherent resonance fluorescence triplet. These results demonstrated the great effectiveness of the present system for the study of the interaction between light and cold atoms. Higher-order processes, such as cooperative effect in resonance fluorescence [18–21] and mesoscopic fluctuations originated from a multi-level structure of atoms [22], can now be viewed as a interesting research subject.

#123497 - $15.00 USD Received 29 Jan 2010; revised 9 Feb 2010; accepted 9 Feb 2010; published 15 Mar 2010

Acknowledgments

This work was supported by Grants-in-Aid for Scientific Research from MEXT.

#123497 - $15.00 USD Received 29 Jan 2010; revised 9 Feb 2010; accepted 9 Feb 2010; published 15 Mar 2010